Seminar title: Towards precision neutrino mass spectroscopy using atoms/molecules

Seminar speaker: M. Yoshimura

Center of Quantum Universe, Okayama University, Japan

With the expected small neutrino mass of a fraction of eV the energy mismatch becomes a serious problem in planned neutrino experiments using conventional nuclear targets where several MeV energy is released. On the other hand, with the advent of remarkable technological innovations, manipulation of atoms and molecules may contribute greatly to fundamental physics. Neutrino physics may become one of these areas.

We have proposed the precision neutrino mass spectroscopy using atomic targets whose closeness of the released energy to expected neutrino masses is a great advantage. The relevant process of our interest is cooperative (and coherent, called macro-coherent subsequently) atomic de-excitation; $|e\rangle \to |g\rangle + \gamma + \nu_i\nu_j$ where $\nu_{i(j)}, i, j = 1, 2, 3$ is one of neutrino mass eigenstates. Measured quantities are photon spectrum rates and parity non-conserving quantities.

To obtain a measurable rate of the process, it is crucial to develop the macro-coherence [1], [2], a new kind of coherence that involves both atomic polarization and fields. The measured photon energy in the de-excitation has a continuous spectrum below $\omega_{ij} = \frac{\epsilon_{eg}}{2} - \frac{(m_i+m_j)^2}{2\epsilon_{eg}}$. (with $\epsilon_{eg} = \epsilon_e - \epsilon_g$ the atomic energy difference of initial and final states). Determination of the threshold location (decomposition into neutrino mass eigen-states) is made possible by precision of irradiated laser frequencies, and not by resolution of detected photon energy.

The macro-coherently amplified radiative emission of neutrino pair has been coined RENP (radiative emission of neutrino pair) [1], [3] and this method can ultimately determine all three masses, the nature of neutrino masses (Dirac vs Majorana distinction), and the new Majorana source of CPV phases. It was also recently found [4] that relic cosmic neutrino of 1.9 K can be measured if one knows the smallest neutrino mass with some precision.

We shall explain both theoretical aspects of the experimental principle and the present status of experiments of our group, which has succeeded in demonstrating the macro-coherent amplification mechanism in weak QED process [5].

References

[1] A. Fukumi et al., *Progr. Theor. Exp. Phys.***2012, 04D002**; arXiv1211.4904v1[hep-ph](2012) and references cited therein.

[2] M. Yoshimura, N. Sasao, and M. Tanaka, *Phys. Rev* **A86**,013812(2012).

[3] M. Yoshimura and N. Sasao, Phys. Rev. D **89**, 053013 (2014).

[4] M. Yoshimura, N. Sasao, and M. Tanaka, *Experimental method of detecting relic neutrino by atomic de-excitation*, arXiv: 1409.3648v1[hep-ph] (2014).

[5] Y. Miyamoto et al, arXiv:1406.2198v2 [physics.atom-ph] (2014): Prog. Theor. Exp. Phys. 113C01 (2014).

Towards Neutrino mass spectroscopy using atoms/molecules

M. Yoshimura @Okayama University

- Why atoms for neutrino physics
- Unique way to distinguish Majorana from Dirac, and to determine the smallest neutrino mass
- Relic 1.9 K neutrino detection is feasible

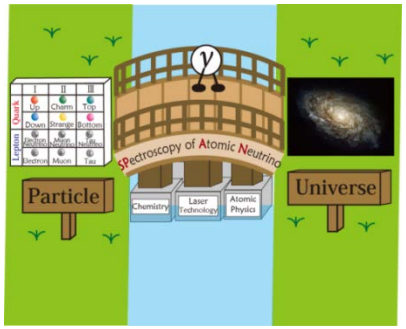

SPAN project

Search for the missing link of micro- and macro- worlds

Collaborators

Staff:

K. Yoshimura (Cosmic Ray)
N. Sasao (Particle Phys.)
N. Nakano (Particle Phys.)
M. Yoshimura (Theory)
S. Uetake (Quant. Elec.)
A. Yoshimi (Nucl. Phys.)
Y. Miyamoto (Chem.)
T. Masuda (Particle Phys)
H. Hara (Atomic Phys.)

Students:

Y. Tsutsumi
T. Iwasaki

Okayama Univ.

Introduction

- What have been, and have not been, determined in neutrino experiments so far

- Remaining important questions on neutrino properties to probe physics beyond the standard theory and cosmology

Present status of neutrino physics

- Oscillation experiments
  - Finite mass
  - Flavor mixing
  - Only mass-squared difference can be measured.

$$U = VP, \tag{A8}$$

where

$$V = \begin{bmatrix} c_{12}c_{13} & s_{12}c_{13} & s_{13}e^{-i\delta} \\ -s_{12}c_{23} - c_{12}s_{23}s_{13}e^{i\delta} & c_{12}c_{23} - s_{12}s_{23}s_{13}e^{i\delta} & s_{23}c_{13} \\ s_{12}s_{23} - c_{12}c_{23}s_{13}e^{i\delta} & c_{12}c_{23} - s_{12}s_{23}s_{13}e^{i\delta} & c_{23}c_{13} \end{bmatrix}, \tag{A9}$$

with $c_{ij} = \cos\theta_{ij}$ and $s_{ij} = \sin\theta_{ij}$. The diagonal unitary matrix P may be expressed by

$$P = \mathrm{diag.}(1, e^{i\alpha}, e^{i\beta}), \tag{A10}$$

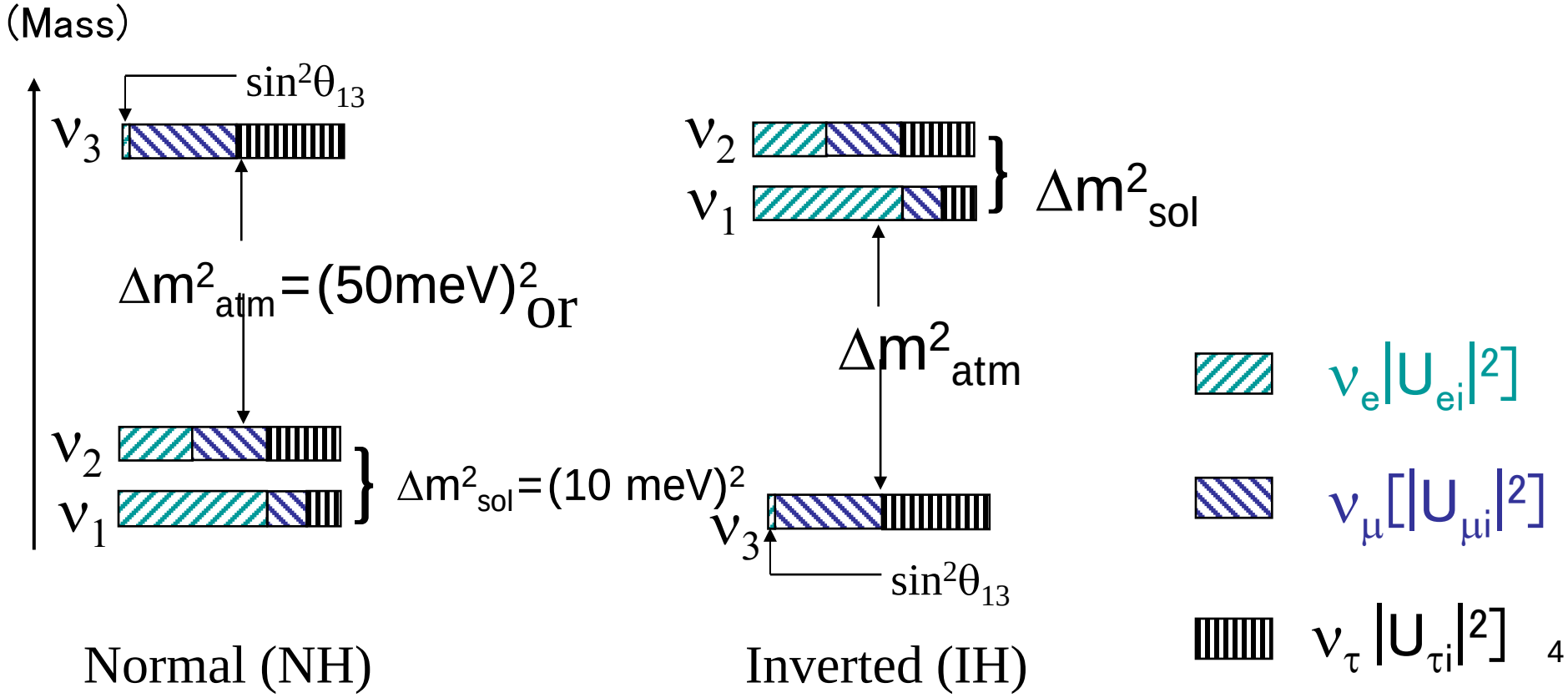

Important questions left in neutrino physics

- Absolute mass scale and the smallest mass (oscillation experiments are sensitive to mass squared differences alone)
- Majorana vs Dirac distinction
- CPV phase （Majorana case has 2 extra phases）

$$\alpha\,,\ \beta\,,\ \delta\ (\mathrm{KM-type})$$

These are relevant to explanation of matter-antimatter imbalance of universe.

We wish to experimentally achieve all of these goals.

Our Okayama group has proposed an entirely new method using atoms, initiated R&D works and succeeded in establishing the huge rate enhancement in QED process, along with theoretical works.

Present status of nuclear target experiments

1. Majorana nature： neutrino-less double beta decay

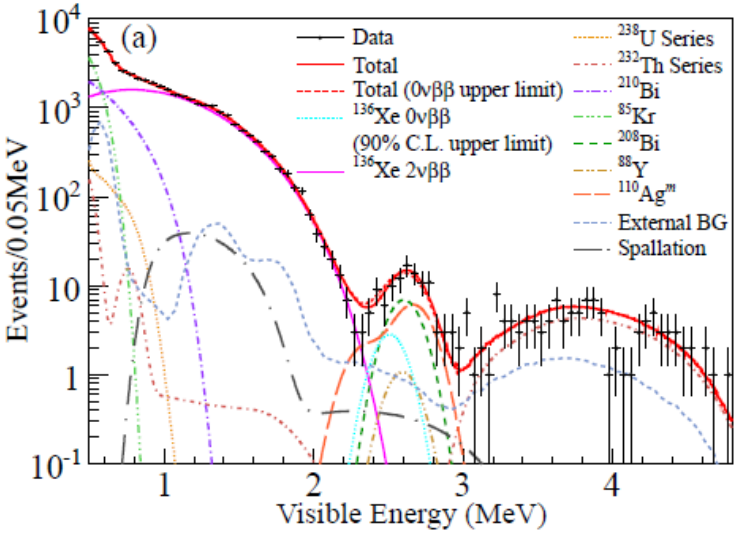

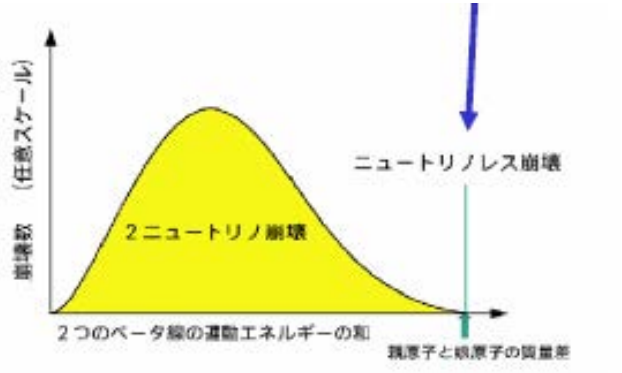

2. Absolute mass

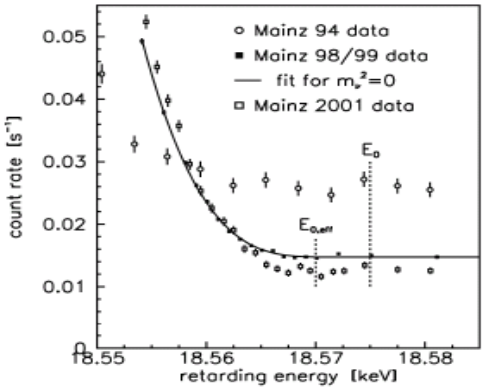

Fig. 20. Averaged count rate of the 98/99 data (filled squares) with fit for $m^2(\nu_e) = 0$ (line) and the 2001 data (open squares) in comparison with previous Mainz data from phase I (open circles) plotted as function of the retarding potential near the endpoint E_0.

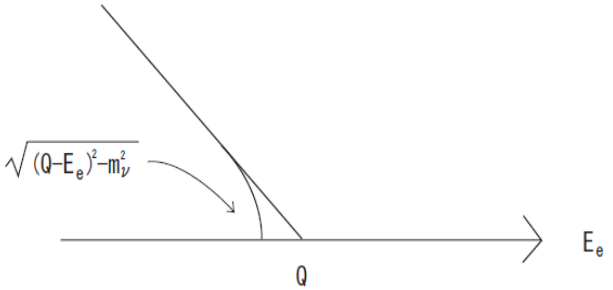

Significance of Majorana neutrinos

- Suppose that neutral leptons consist of 4 components like all other quarks and leptons, the other 2-componet neutral lepton having a much larger mass of Majorana-type than the ordinary neutrino
- Plausible scenario of lepto-genesis

Heavy Majorana decay resposibe for generation of lepton asymmetry, being converted to baryon asymmetry via strong electroweak B, L violation keeping B-L conserved.

Prerequisite: ordinary neutrinos are also Majorana. New CPV sources related to heavy partners of mass >> Fermi scale

- Seesaw mechanism and an important step for construction of grand unified theory

$$\frac{m^2}{M}$$

Lepto-genesis

- Leading theory to explain the matter-antimatter imbalance of our universe
- Prerequisite: lepton number violation or Majorana type of mass, CP violation
- Sensitivity to low energy parameters Davidsson-Ibarra, NPB648, 345(2003)

CP asymmetry in leptogeneis

$$\approx \frac{3y_1^2}{4\pi}\left(-2(\frac{m_3}{m_2})^3 s_{13}^2 \sin 2(\delta+\alpha-\beta)+\frac{m_1}{m_2}\sin(2\alpha)\right)$$

+ (high energy phases inaccessible in low energy experiments)

Ours are sensitive to α, $\beta-\delta$; the same as in lepto − genesis

Majorana vs Dirac equations:

Majorana eq. : particle=antiparticle

$$(i\partial_t - i\vec{\sigma}\cdot\vec{\nabla})\varphi = im\sigma_2\varphi^*$$

$$\varphi_{\vec{p},h}(x) = c(\vec{p},h)e^{-ip\cdot x}u(\vec{p},h) + c^\dagger(\vec{p},h)e^{ip\cdot x}\sqrt{\frac{E_p+hp}{E_p-hp}}(-i\sigma_2)u^*(\vec{p},h)\,,$$

$$u(\vec{p},h) = \frac{1}{2}\sqrt{\frac{E_p-hp}{pE_p(p+hp_3)}}\begin{pmatrix} p+hp_3 \\ h(p_1+ip_2)\end{pmatrix}.$$

2 neutrino wave functions are anti-symmetrized due to the Pauli exclusion principle

Dirac eq.: degenerate 2 Majorana and lepton number conservation

$$(i\partial_t - i\vec{\sigma}\cdot\vec{\nabla})\varphi = m\chi\,, \quad (i\partial_t + i\vec{\sigma}\cdot\vec{\nabla})\chi = m\varphi$$

2-component in weak process involved

$$\psi_D = (1-\gamma_5)\psi/2$$

$$\psi_D = b(\vec{p},h)e^{-ip\cdot x}u(\vec{p},h) + d^\dagger(\vec{p},h)e^{ip\cdot x}\sqrt{\frac{E_p+hp}{E_p-hp}}(-i\sigma_2)u^*(\vec{p},h)$$

Particle annihilation Anti-particle creation

Majorana phase dependence

- Pair emission current at cross threholds

$$\langle (ip_1 h_1\,, jp_2 h_2)|j_\nu|0\rangle = \xi_i^*\xi_j e^{i(p_1+p_2)\cdot x} v_1^\dagger \sigma u_2 - \xi_i\xi_j^* e^{i(p_1+p_2)\cdot x} v_2^\dagger \sigma u_1$$
$$= e^{i(p_1+p_2)\cdot x}\left(i\Im\xi_i^*\xi_j (v_1^\dagger\sigma u_2 + v_2^\dagger \sigma u_1) + \Re\xi_i^*\xi_j (v_1^\dagger\sigma u_2 - v_2^\dagger\sigma u_1)\right)$$

$$\xi_i^*\xi_j = U_{ei}^* U_{ej} = c_{ij}^{(0)}\,, \quad U_{e1} = c_{12}c_{13}\,,\ U_{e2} = s_{12}c_{13}e^{i\alpha}\,,\ U_{e3} = s_{13}e^{i\beta}$$

Unless $(v_1^\dagger\sigma u_2 + v_2^\dagger\sigma u_1)$ and $(v_1^\dagger\sigma u_2 - v_2^\dagger\sigma u_1)$ are orthogonal, T-reversal violation $\propto \Im\xi_i^*\xi_j \Re\xi_i^*\xi_j$ can be measured, and all Majorana phases $\alpha\,,\beta$ are measurable. Non-orthogonality holds for $i \neq j$, or $m_i \neq m_j$.

$$\cos(2\alpha)\,, \quad \cos 2(\beta-\delta)\,, \quad \text{at } (12),(13),(23) \text{ thresholds}$$

Access to independent phase combination, unlike its linear combination in neutrino-less double beta decay

$$\left|\sum_i m_i U_{ei}^2\right|^2 = m_3^2 s_{13}^4 + m_2^2 s_{12}^4 c_{13}^4 + m_1^2 c_{12}^4 c_{13}^4 + 2m_1 m_2 s_{12}^2 c_{12}^2 c_{13}^4 \cos(2\alpha)$$
$$+ 2m_1 m_3 s_{13}^2 c_{12}^2 c_{13}^2 \cos 2(\beta-\delta) + 2m_2 m_3 s_{13}^2 s_{12}^2 c_{13}^2 \cos 2(\alpha-\beta+\delta),$$

Relevant atomic process to us

Radiative Emission of Neutrino Pair (RENP) from metastable atomic levels

- Process undoubtedly existing in standard theory, assuming finite neutrino masses

- Possible to amplify otherwise small rates by developing macro-coherence of a twin process

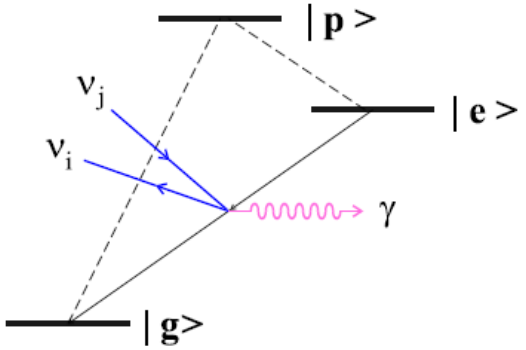

Expected RENP rate

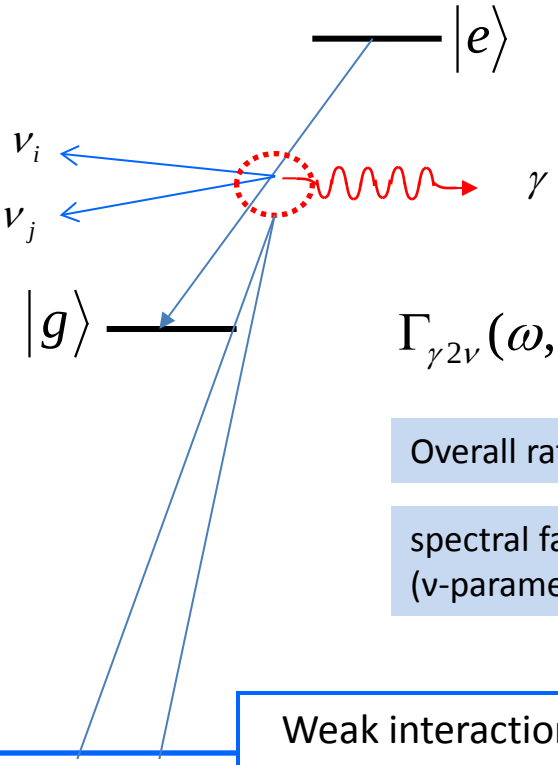

$$I(\omega)$$

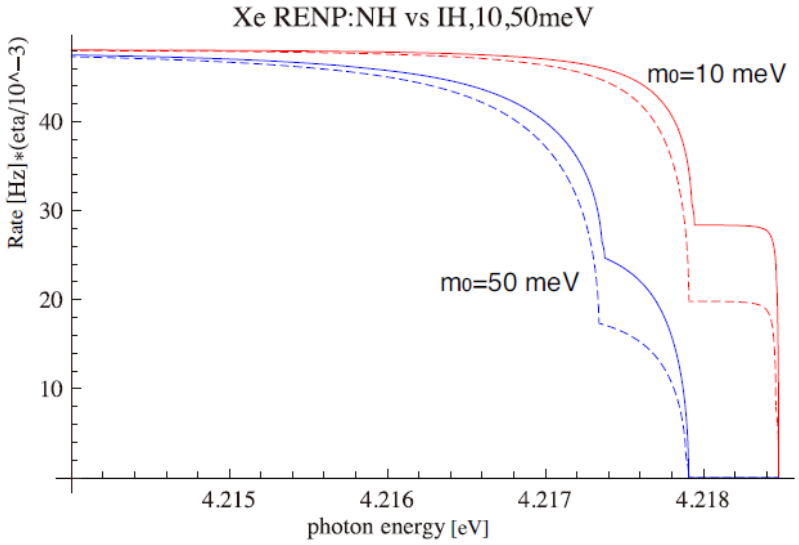

$$\Gamma_{\gamma 2\nu}(\omega,t) = \Gamma_0\, I(\omega)\, \eta_\omega(t)$$

Overall rate

spectral factor (ν-parameter)

activity factor in target (macroscopic pol. x field)

$$\Gamma_0 \sim 40\mathrm{Hz}\cdot\left(n/(7\times10^{19}\,\mathrm{cm}^{-3})\right)^3\cdot\left(V/(10^2\,\mathrm{cm}^3)\right)$$

Large rate enhancement for heavy atoms

Weak interaction process in atomic transition

Neutral current

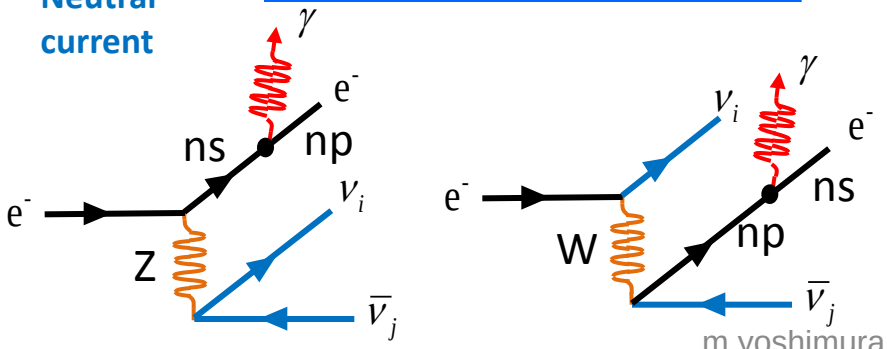

Neutrino pair from nucleus

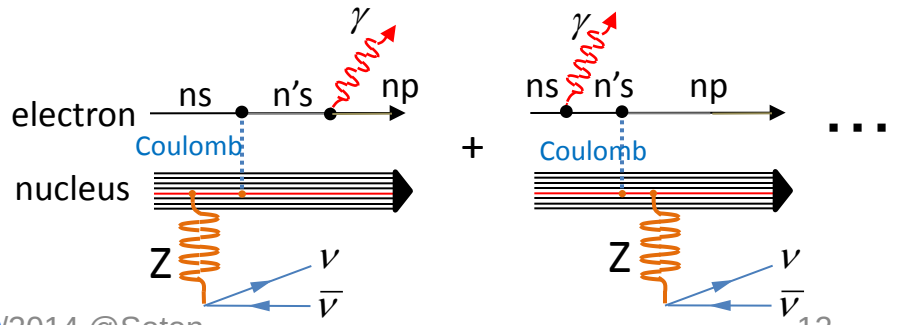

Rate amplification by macroscopic coherence

- Super-radiance coherent volume (Dicke)
  - In case of SR, coherent volume is proportional to $\lambda^2 L$.
  - Phase decoherence time (T_2) must be longer than T_{SR}

$$\text{Rate} \propto \left| \sum_j^N e^{i\vec{k}\cdot\vec{r}_j} M_{atm} \right|^2 \propto N^2 \quad \left(\text{for } |r_j - r_l| \leq \lambda \right)$$

- For a process with plural outgoing particles
  - Phase matching condition (momentum conservation) is satisfied.
  - Coherent volume is not limited by λ., can be macroscopic.

$$\text{Rate} \propto \left| \sum_j^N e^{i(\vec{k}_1+\vec{k}_2+\vec{k}_3)\cdot\vec{r}_j} M_{atm} \right|^2 \propto N^2 \quad \left(\text{for } \vec{k}_1 + \vec{k}_2 + \vec{k}_3 = 0 \right)$$

Superradiance: 2 level and 1 photon case

1916—1997

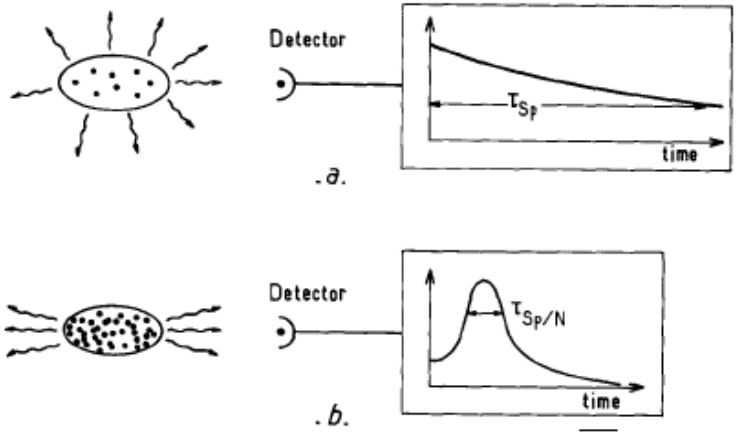

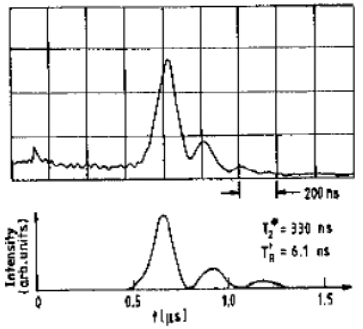

Figure 2.2. Oscilloscope trace of the super-radiance pulse observed by Skribanowitz *et al* [SHMF73] in HF gas at 84 μm ($J = 3 \rightarrow 2$), pumped by the $R_1(2)$ laser line, and the theoretical fit. The parameters are: pump intensity $I = 1$ kW cm^{-2}, $p = 1.3$ mTorr, $L = 100$ cm. The small peak on the oscilloscope trace at $t = 0$ is the 3 μm pump pulse, highly attenuated.

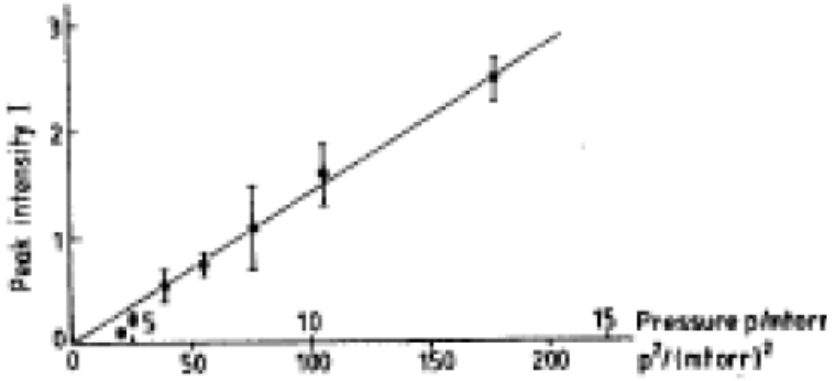

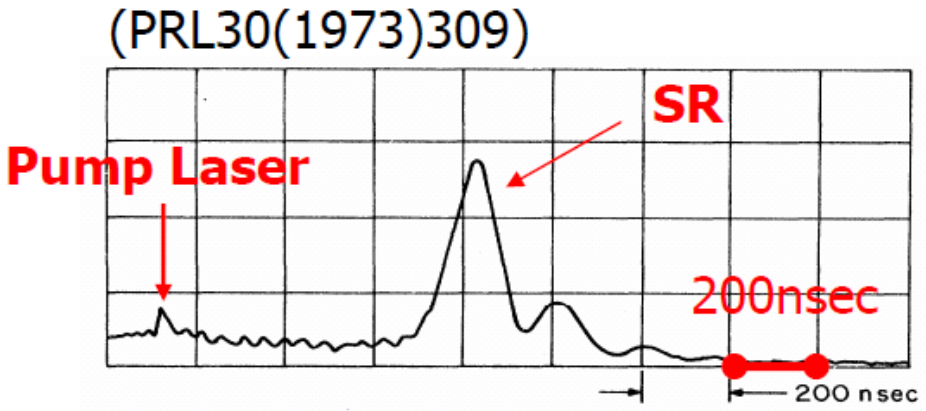

Rate enhanced by N

Delayed enhanced signal accompanied by ringing

Paired Super-Radiance (PSR) important to develop large rates for RENP (also to prove the principle of macro-coherence)

- Macro-coherent amplification
  - A new type of coherent phenomena
  - Should be established experimentally
- Two photon emission process

$$|e\rangle \rightarrow |g\rangle + \gamma + \gamma$$

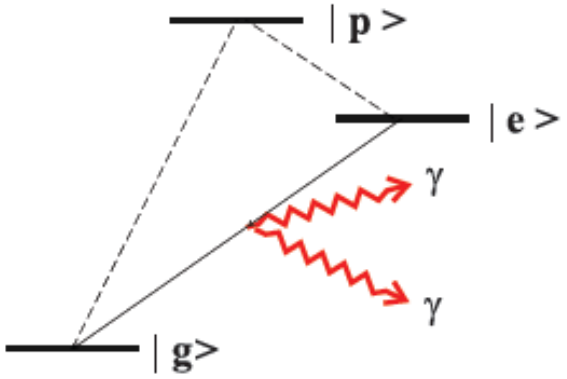

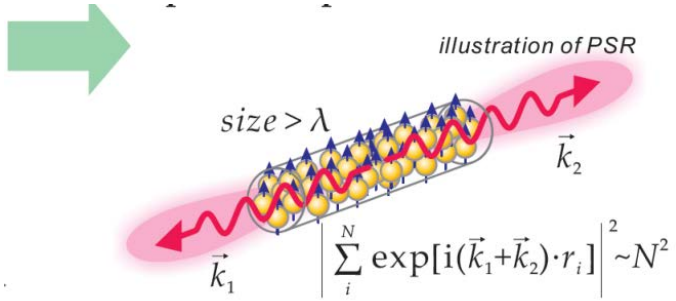

- Paired Super-Radiance
  - QED instead of weak process
  - Good experimental signature; i.e. back-to-back radiations with same color.

Some details on simulations of macro-coherence development

Effective 2-level model for trigger and medium evolution

2 level interaction with field

$$\frac{d}{dt}\begin{pmatrix} c_e \\ c_g \end{pmatrix} = -i\mathcal{H}\begin{pmatrix} c_e \\ c_g \end{pmatrix}, \quad -\mathcal{H} = 2\begin{pmatrix} \mu_{ee} & 2e^{i\epsilon_{eg}}\mu_{ge} \\ 2e^{-i\epsilon_{eg}}\mu_{ge} & \mu_{gg} \end{pmatrix} E^2$$

Stark shifts : 2×2 Hamiltonian

Ba $\begin{pmatrix} 6.0 & 2.1 \\ 2.1 & 16 \end{pmatrix} \mathrm{GHz}\,\frac{|E|^2}{10^6 \mathrm{W mm^{-2}}}$

Yb $\begin{pmatrix} -1.2\times10^{-7} & 1.7\times10^{-4} \\ 1.7\times10^{-4} & 6.6 \end{pmatrix} \mathrm{GHz}\,\frac{|E|^2}{10^6 \mathrm{W mm^{-2}}}$

Xe $\begin{pmatrix} -8.4\times10^{-11} & 1.5\times10^{-5} \\ 1.5\times10^{-5} & 0.22 \end{pmatrix} \mathrm{GHz}\,\frac{|E|^2}{10^6 \mathrm{W mm^{-2}}}$

Ca^+ $\begin{pmatrix} 10 & 2.5 \\ 2.5 & 4.5 \end{pmatrix} \mathrm{GHz}\,\frac{|E|^2}{10^6 \mathrm{W mm^{-2}}}$

pH_2 $\begin{pmatrix} 0.27 & 0.16 \\ 0.16 & 0.22 \end{pmatrix} \mathrm{GHz}\,\frac{|E|^2}{10^6 \mathrm{W mm^{-2}}}$

$$\mu_{ee} = 2\sum_j \frac{d_{je}^2 E_{je}}{E_{je}^2 - \omega^2}, \quad \mu_{gg} = 2\sum_j \frac{d_{jg}^2 E_{jg}}{E_{jg}^2 - \omega^2}, \quad d_{ij} = \sqrt{3\pi\frac{\gamma_{ij}}{E_{ij}^3}}$$

$$\mu_{eg} = \sum_j \frac{d_{je}d_{jg}}{E_c - \delta\omega}, \quad \mu_{ge} = \sum_j \frac{d_{je}d_{jg}}{E_c + \delta\omega}.$$

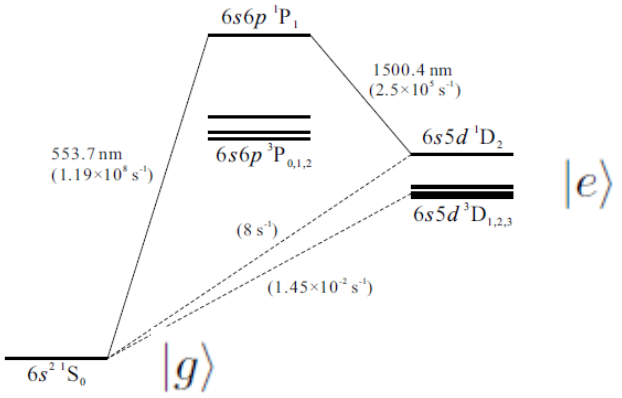

Ba

Maxwell-Bloch equation for PSR simulations: 1+1 dim

Bloch equation for medium

$$\vec{R} = \mathrm{tr}\ \rho\vec{\sigma} = \langle\psi|\vec{\sigma}|\psi\rangle$$

$$\partial_t R_1 = (\mu_{ee} - \mu_{gg})E^+E^-R_2 - i\mu_{ge}(e^{i\epsilon_{eg}}E^+E^+ - e^{-i\epsilon_{eg}}E^-E^-)R_3 - \frac{R_1}{T_2}\,,$$

$$\partial_t R_2 = -(\mu_{ee} - \mu_{gg})E^+E^-R_1 + \mu_{ge}(e^{i\epsilon_{eg}}E^+E^+ + e^{-i\epsilon_{eg}}E^-E^-)R_3 - \frac{R_2}{T_2}\,,$$

$$\partial_t R_3 = \mu_{ge}\left(i(e^{i\epsilon_{eg}}E^+E^+ - e^{-i\epsilon_{eg}}E^-E^-)R_1 - (e^{i\epsilon_{eg}}E^+E^+ + e^{-i\epsilon_{eg}}E^-E^-)R_2\right) - \frac{R_3 + n}{T_1}\,.$$

T_2 phase relaxation time, T_1 population decay time

Field equation

$$(\partial_t^2 - \vec{\nabla}^2)\vec{E} = \vec{\nabla}^2\mathcal{D}\vec{E}\,,$$

$$-\mathcal{D}\vec{E}^+ = \left(\frac{\mu_{ee}+\mu_{gg}}{2}n + \frac{\mu_{ee}-\mu_{gg}}{2}R_3\right)\vec{E}^+ + \mu_{ge}e^{-i\epsilon_{eg}t}(R_1 - iR_2)\vec{E}^-\,.$$

SVEA (Slowly Varying Envelope Approximation)

$$E = \frac{1}{2}\left(e^{-i\omega_1(t-x)}E_R + e^{-i\omega_2(t+x)}E_L + (\mathrm{h.c.})\right)\,, \qquad \omega_1 + \omega_2 = \epsilon_{eg}$$

complex amplitudes $E_R(x,t), E_L(x,t)$ slowly varying in 1+1 spacetime

- Coupled system of field and medium polarization highly non-linear

PSR simulations for two counter-propagating modes

Explosive PSR with initial coherence

para-H2 $n = 1 \times 10^{21}\,\mathrm{cm}^{-3}$, $L = 30\,\mathrm{cm}$, $T_1 = 1\,\mu\mathrm{s}$, $T_2 = 10\,\mathrm{ns}$

Coherent initial state: $r_1 = 1,\ r_2 = r_3 = 0$

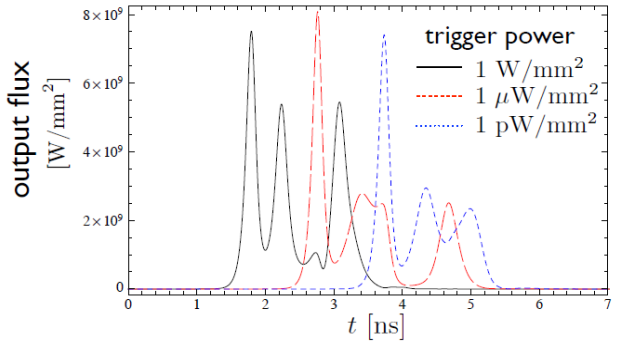

Minoru TANAKA

8

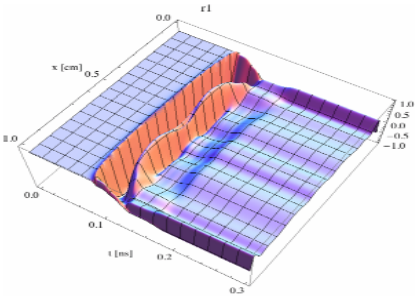

Figure 6: Spacetime profile of r_1 for the 1 Wmm^{-2} case of Fig(3).

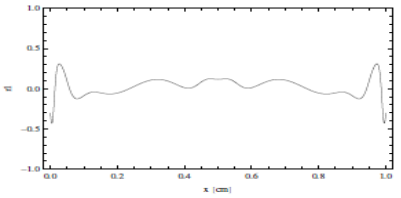

Figure 7: Spatial profile of r_1 at the latest time, 0.3 ns after trigger irradiation, of Fig(6).

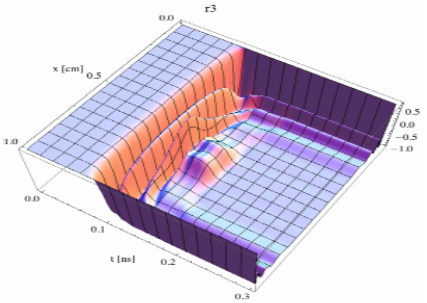

Figure 8: Spacetime profile of r_3 for the 1 Wmm^{-2} case of Fig(3).

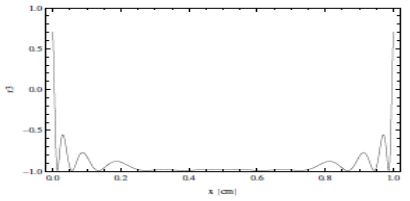

Figure 9: Spatial profile of r_3 at the latest time, 0.3 ns after trigger irradiation, of Fig(8).

Explosive event:
Most energy stored in upper level is released in < 1ns

Weak linear regime of PSR

- In reality,

finite target size

short relaxation

time target number density not large enough etc.

May lead to termination of complete macro-coherence development. In this case its rate given by $\propto n\rho_{eg}$

RENP process from developed macro-coherence

- RENP rate amplified by both medium polarization and two frequency fields, stored by large amount

- RENP occurs perturbatively under this circumstance, hence reliably calculable except the activity factor, η

Radiative emission of neutrino pair (RENP)

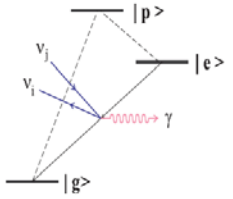

Fig. 1 Λ−type atomic level for RENP $|e\rangle \to |g\rangle + \gamma + \nu_i\nu_j$ with ν_i a neutrino mass eigenstate. Dipole forbidden transition $|e\rangle \to |g\rangle + \gamma + \gamma$ may also occur via weak M1× E1 couplings to virtual intermediate state $|p\rangle$.

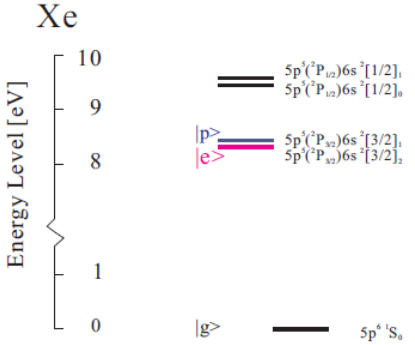

$$\Gamma = \Gamma_0\ \mathrm{I}(\omega)\ \eta(t)$$

$$2^- \to 0^+$$

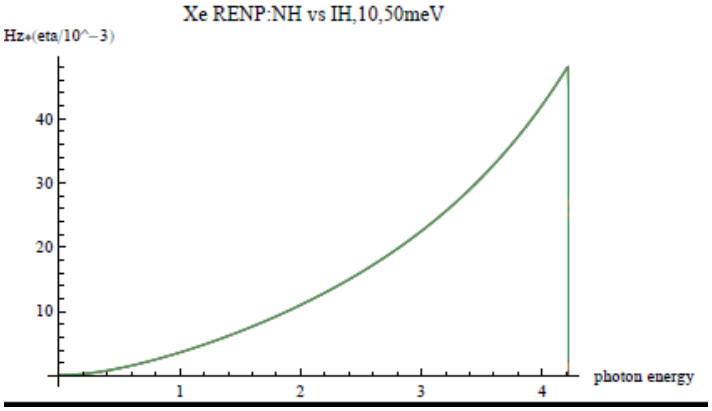

Six pair production thresholds of mass eigen states

$$\omega_{ij} = \frac{\epsilon_{eg}}{2} - \frac{(m_i + m_j)^2}{2\epsilon_{eg}}$$

Due to energy and momentum conservation
Resolved by precision of trigger lasers

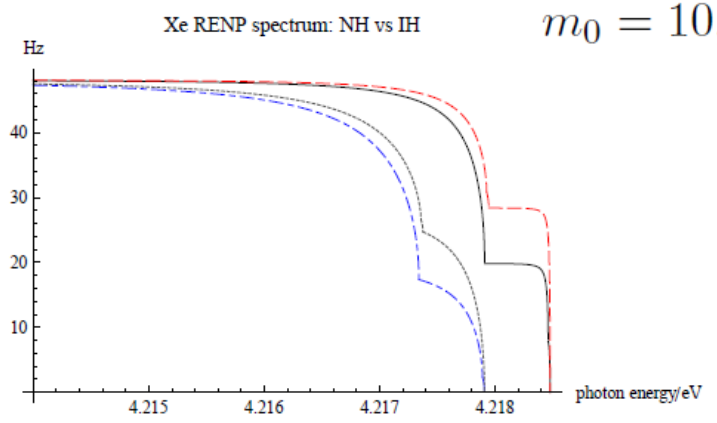

$m_0 = 10, 50\mathrm{meV}$

IH

NH

Nuclear monopole rates

- Pair emission from nucleus (monopole) gives the largest rates

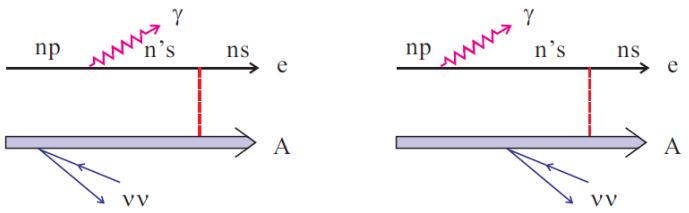

Figure 3: RENP diagrams 3 for alkali atoms.

$$Q_W^2 Z^{8/3}$$

$$Q_w \sim N - 0.044Z$$

Nuclear coherence effect

Spectrum rates for gas Xe

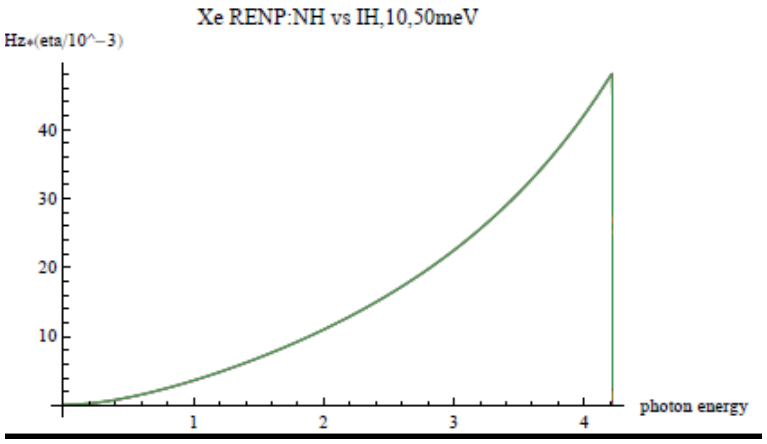

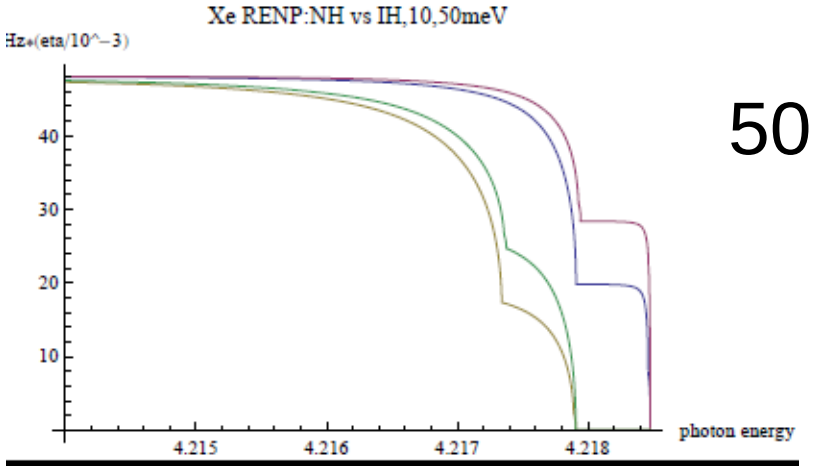

50 Hz

Dirac vs Majorana & CP phases

We need to go to the lower energy (smaller level spacing) to see M/D distinction and CPV phases.

Eeg= 0.429 eV
Epg= 0.446 eV

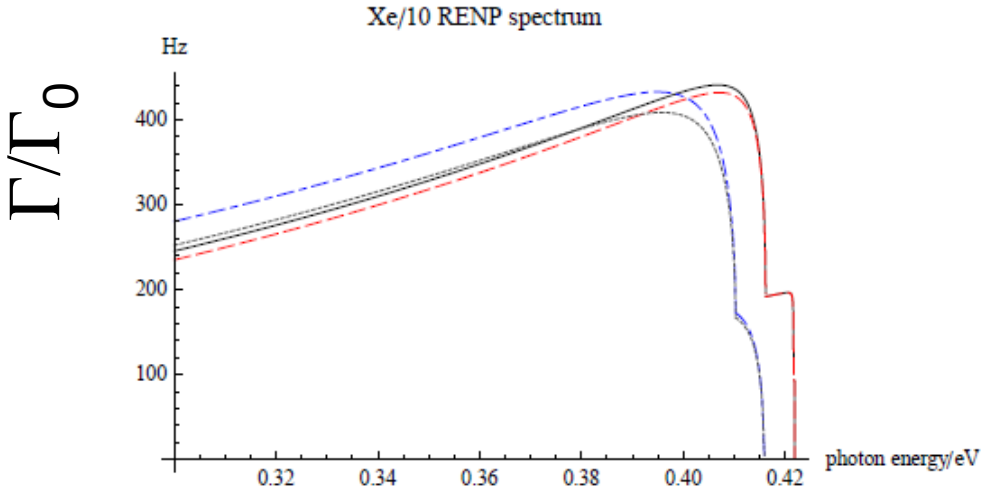

More than 10% possible

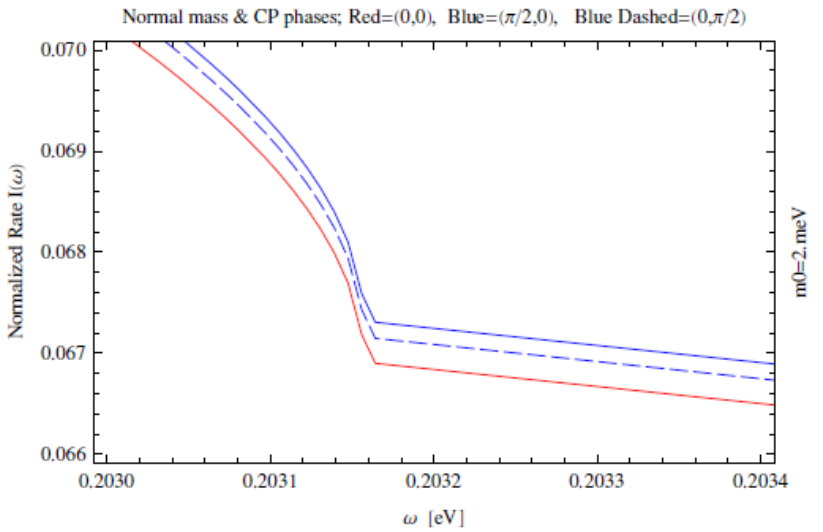

A few % level

Parity violating effects and asymmetric rates calculated: proof of involved weak interaction and important to increase S/N ratio

1. asymmetry under the magnetic field reversal,
2. asymmetry under the reversal of trigger photon circular polarization

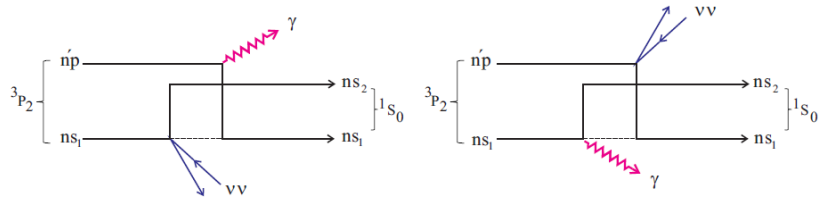

Figure 1: Parity odd contribution of valence electron exchange. Neutrino pair emission contains the PO part of vertex, as described in the text.

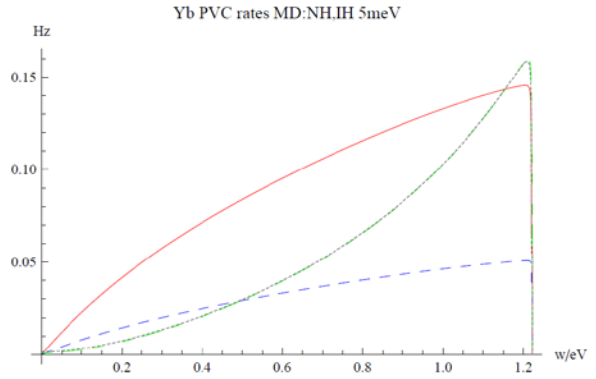

Figure 8: ${}^3P_2, J = 2, M_J = 1$ Yb PC rates, PV rate differences. Zeeman mixing amplitude 5×10^{-6} (corresponding to the magnetic field **), $\eta_\omega(t) = 1$, $n = 10^{22}\text{cm}^{-3}$, and 10^2cm^3 are assumed. Majorana NH PV in solid red, M-IH PV in dashed blue, M-NH PC rate divided by 50 in dash-dotted green, and M-IH/50 in dotted black (degenerate with M-NH PC).

PV rate much smaller than PC rate

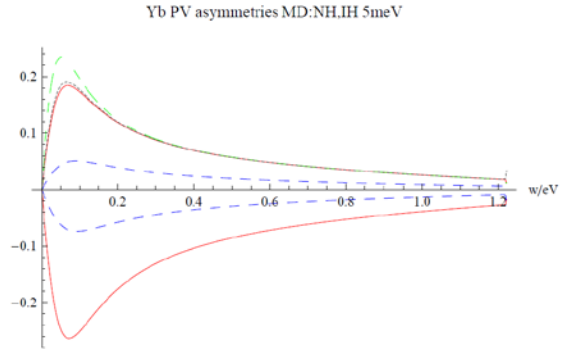

Figure 11: ${}^3P_2$Yb PV asymmetries vs photon energy. Zeeman mixing amplitude 5×10^{-6}, $\eta_\omega(t) = 1$, $n = 10^{22}\text{cm}^{-3}$, and a target volume 10^2cm^3 assumed. In the positive side the Majorana case of PV asymmetry under polarization reversal for NH is depicted in solid red, M-IH case in dashed blue, D-NH in dash-dotted green and the Dirac case for IH in dotted black. In the negative side PV asymmetry under the field reversal is plotted; M-NH and D-NH in solid red, and M-IH and D-IH in dashed blue, all assuming the smallest neutrino mass 5 meV.

MD distinction possible by measurement of PV asymmetry

Detection of relic neutrinos of 1.9 K

Recent work with N. Sasao and M. Tanaka
arXiv: 1409.3648

- Direct remnant at a few seconds after the big bang
- Prove that neutrinos were in thermal equilibrium, giving the important basis of light element synthesis such as 4He
- T differs from 2.7K of microwave, because electron-positron annihilation occurred after the neutrino decoupling at a few MeV, heating up matter in equilibrium
- Prediction is firm: (4/11)^(1/3) 2.7 K = 1.9 K, 110cm^-3

- Spectrum distortion by the Pauli blocking caused by ambient relic neutrinos

Neutrino distribution function

$$f(p) = \frac{1}{\zeta e^{\sqrt{p^2+m^2/(z_d+1)^2}/T}+1} \approx \frac{1}{\zeta e^{p/T}+1}$$

$$\zeta = e^{-\mu_d/T_d}, \quad z_d = O(10^{10})$$

Blocking given by 1-f(p)

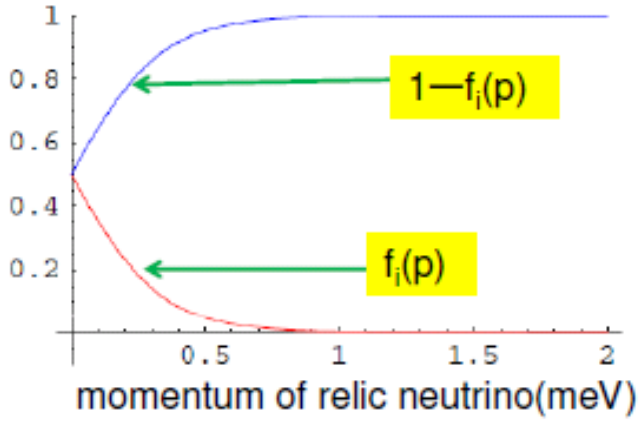

$$F^A_{ij}(\omega;T_\nu) = \frac{1}{8\pi\omega}\int_{E_-}^{E_+} dE_1\, g^A_{ij}(E_1)\cdot\left(1-f(\sqrt{E_1^2-m_i^2})\right)\left(1-\bar{f}(\sqrt{(\epsilon_{eg}-\omega-E_1)^2-m_j^2})\right),$$

$$g^M_{ii}(E) = -E^2+(\epsilon_{eg}-\omega)E+\frac{1}{2}m_i^2-\frac{1}{4}\epsilon_{eg}(\epsilon_{eg}-2\omega)+\delta_M\frac{m_i^2}{2},$$

$$g^S_{ij}(E) = -\frac{1}{3}E^2+\frac{1}{3}(\epsilon_{eg}-\omega)E+\frac{1}{12}\epsilon_{eg}(\epsilon_{eg}-2\omega)-\frac{1}{12}(m_i^2+m_j^2)-\delta_M\frac{m_i m_j}{2},$$

$$E_\pm = \frac{1}{2}\left((\epsilon_{eg}-\omega)\left(1+\frac{m_i^2-m_j^2}{\epsilon_{eg}(\epsilon_{eg}-2\omega)}\right)\pm\omega\Delta_{ij}(\omega)\right), \quad \Delta_{ij}(\omega) = \left\{\left(1-\frac{(m_i+m_j)^2}{\epsilon_{eg}(\epsilon_{eg}-2\omega)}\right)\left(1-\frac{(m_i-m_j)^2}{\epsilon_{eg}(\epsilon_{eg}-2\omega)}\right)\right\}^{1/2}.$$

Temperature measurement possible for RENP ?

Ratio of rates: with to without Pauli blocking

with/without Pauli blocking

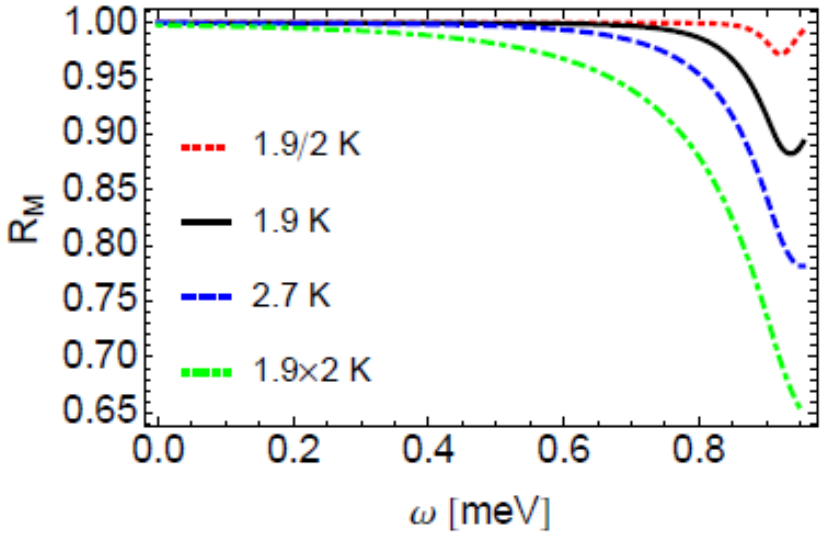

Level spacing 11 meV
Smallest mass 5meV

Difference of distortions
for 1.9 and 2.7 K

10% level

For small level spacing, temperature measurement possible.

Paired Superradiance with pH_2 molecule

PSR with para-Hydrogen molecule (p-H_2)

For observation of PSR …

- One photon forbidden & Two photon allowed
- Initial condition (population / coherence)
- Coherence time

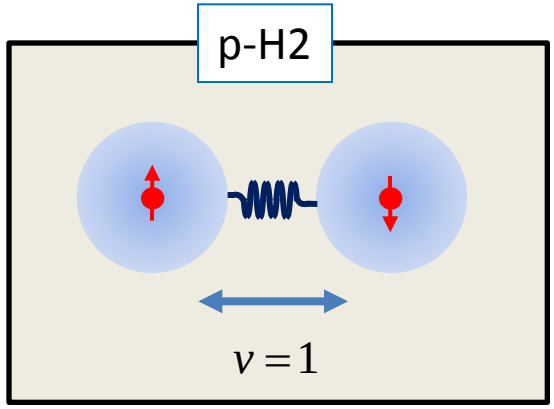

Para-Hydrogen molecule (Spin=0)

- Vibrationally excited state to ground.
- E1 one-photon decay is forbidden.
- Two photon transition is allowed:
  Spontaneous two photon decay is rare process

$$\tau \approx 0.3\times10^{11}\,[\mathrm{s}] \approx 950\,[\mathrm{y}]$$

Rate enhancement

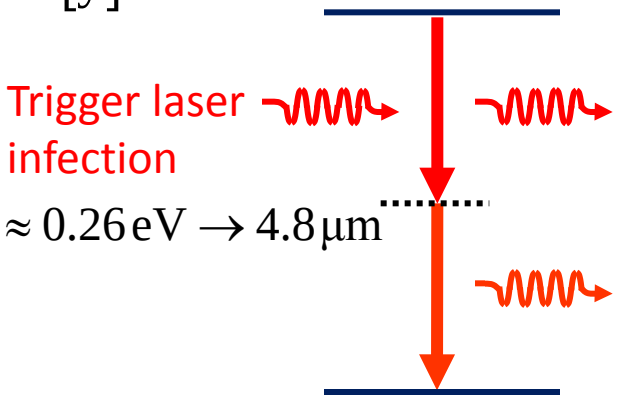

Vibrational transition of homo-nuclear molecules

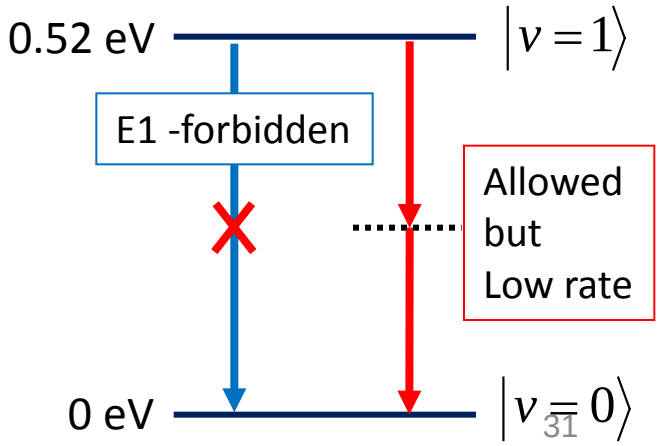

Preparation of initial coherence – Adiabatic Raman -

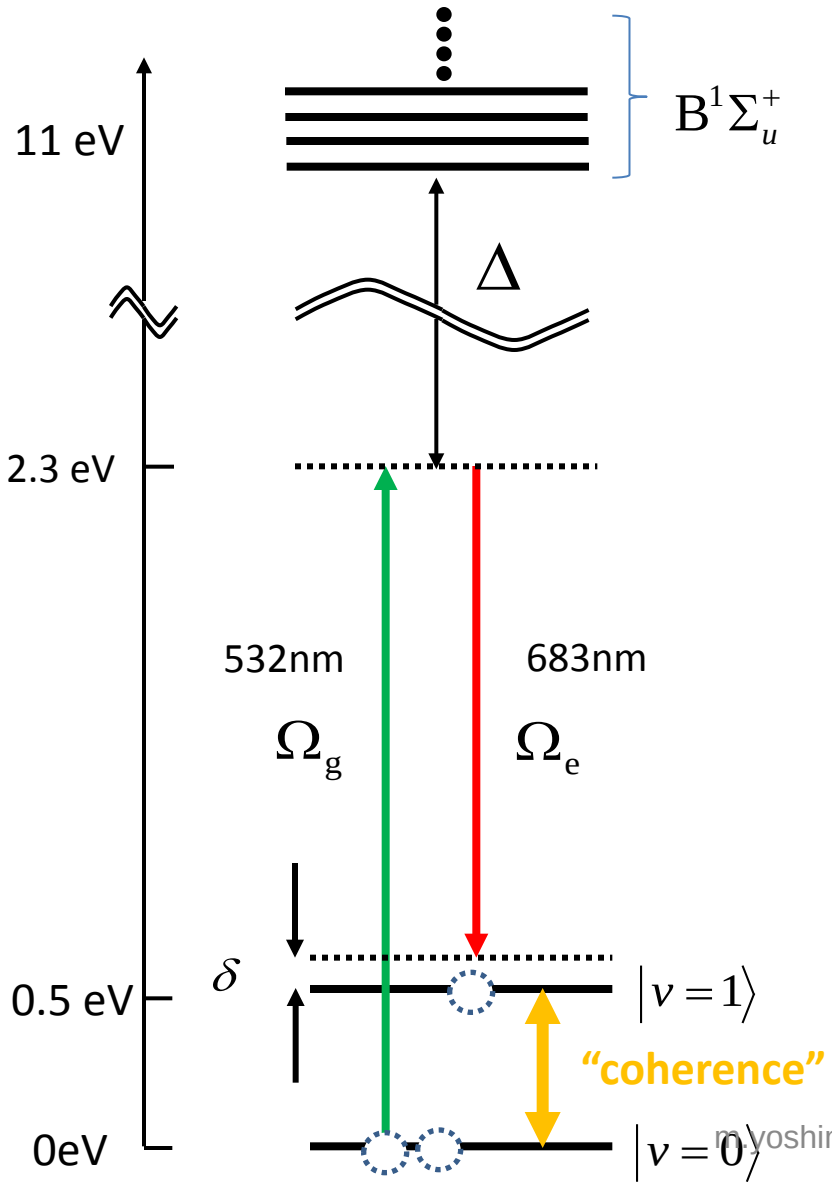

Two laser fields irradiates p-H2

Two photon Rabi frequency $\Omega_{ge} \cong \frac{\Omega_g \Omega_e}{\Delta}$

→ |g> and |e> are mixed with an angle

$$\tan\theta \cong \frac{\Omega_{ge}}{\delta}$$

Non-degenerate Superposition States:

$$|+\rangle = \cos\frac{\theta}{2}|g\rangle + e^{-i\varphi}\sin\frac{\theta}{2}|e\rangle$$

$$|-\rangle = \cos\frac{\theta}{2}|g\rangle - e^{-i\varphi}\sin\frac{\theta}{2}|e\rangle$$

Coherence between |e> and |g>

$$\boxed{|\rho_{eg}| = \frac{1}{2}\sin\theta}$$

p-H2 gas

532nm

683nm

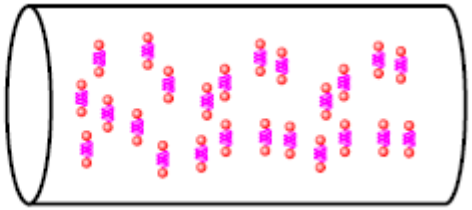

$$|\pm\rangle = |\mathrm{g}\rangle \qquad \theta = 0$$

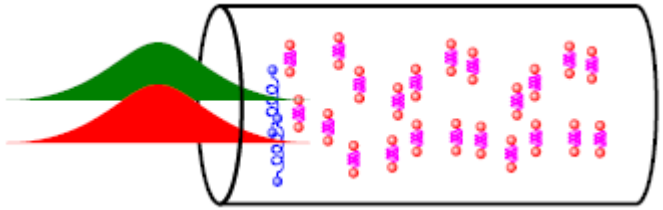

$$|\pm\rangle = \cos\frac{\theta}{2}|\mathrm{g}\rangle \pm e^{-i\varphi}\sin\frac{\theta}{2}|\mathrm{e}\rangle$$

$$\theta \neq 0$$

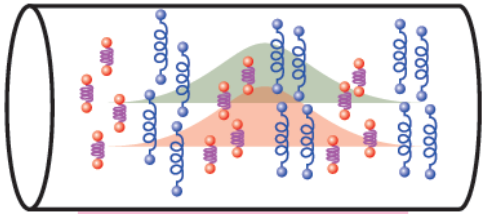

$$|\pm\rangle = \frac{1}{\sqrt{2}}|\mathrm{g}\rangle \pm e^{-i\varphi}\frac{1}{\sqrt{2}}|\mathrm{e}\rangle \qquad \theta = \frac{\pi}{2}$$

$$|\pm\rangle = \cos\frac{\theta}{2}|\mathrm{g}\rangle \pm e^{-i\varphi}\sin\frac{\theta}{2}|\mathrm{e}\rangle$$

$$\theta \neq 0$$

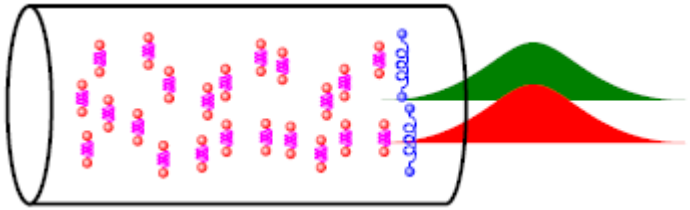

$$\theta = 0 \quad |\pm\rangle = |\mathrm{g}\rangle$$

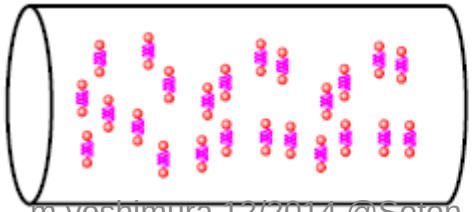

p-H2 target

- pure para-H2 ; o/p ～ 10^-4 – 10^-5
  → Longer phase relaxation time than normal H2
- Cooled down to 77K (LN2)
  → All states in the ground state |v=0>
  → Maximum phase relaxation time (Dicke narrowing)

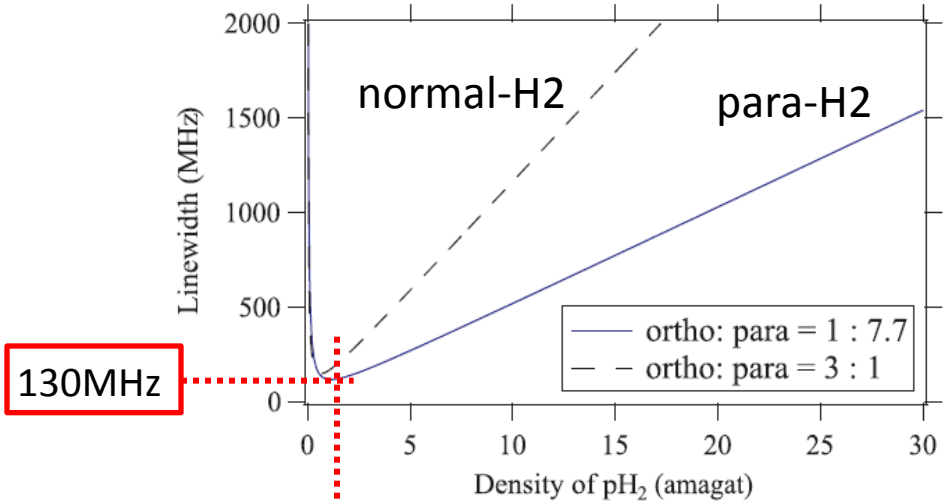

$2.1\text{amagt} \approx 5.6\times10^{19}\,\text{cm}^{-3}$ $60\,\text{kPa}, 77\,\text{K}$

- High damage threshold
- Adiabatic Preparation of large Raman coherence is well studied.
  (S.E. Harris & A.V. Sokolov, Phys. Rev. A 55, R4019 (1997))

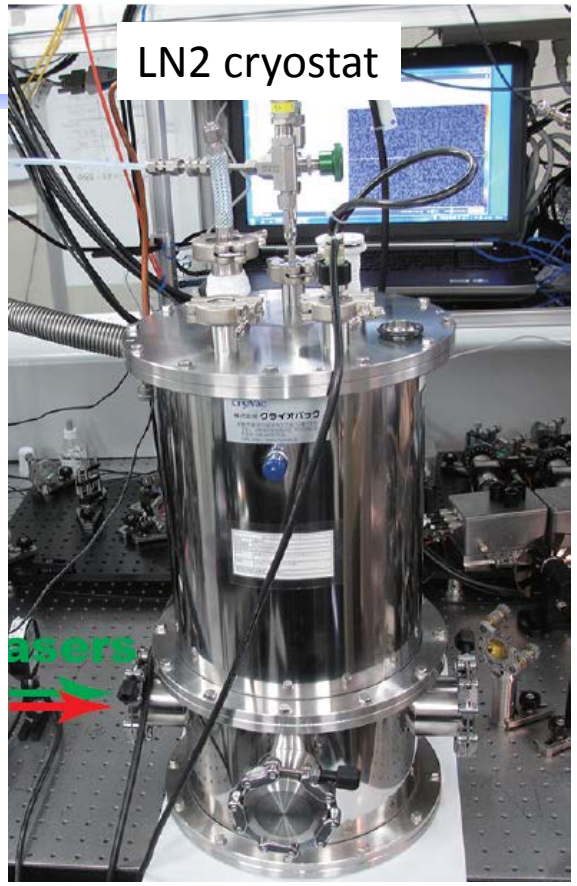

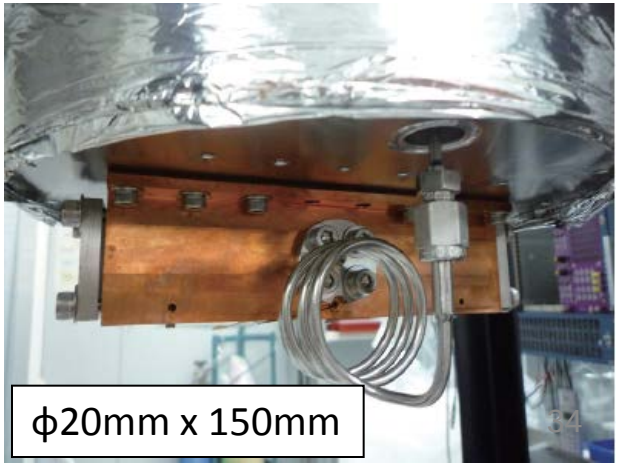

LASER system

Laser requirements

- **To keep adiabatic condition:**

Narrow linewidth $\Delta_{\text{laser}} \le \delta \cong 2\pi \times 130\text{MHz}$; Doppler width

- **Realistic two-photon Rabi frequency:** $\Omega_{ge} = \dfrac{\Omega_g \Omega_e}{\Delta} \sim \delta$

Pump LASER of (5mJ, 6ns-pulse, w0=100μm)
→ 5GW/cm2

$\rightarrow \Omega_{ge} \cong 2\pi \times 170\ \text{MHz}$

v

$\delta\omega_{\text{doppler}} \cong 2\pi \times 130\ \text{MHz}$ (pH2 of T=77K)

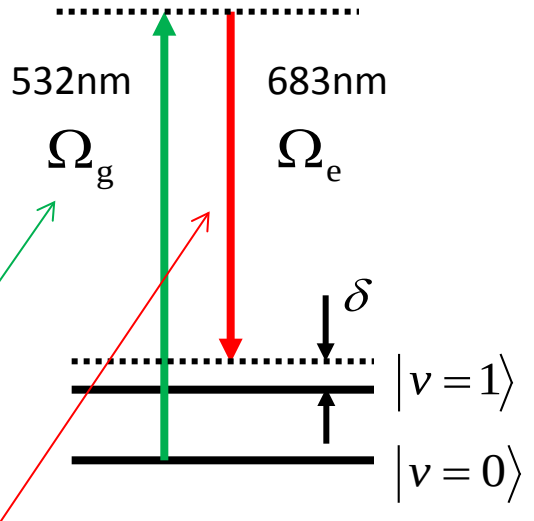

Pump LASER : Nd:YAG(1064nm) + SHG → 532nm
(130mJ, <100MHz)

Stokes LASER of 683nm is needed

Narrow width and high power is commercially not available

Injection seeded OPG (Optical Parametric Generation) + OPA (Amplification)

LASER system

- **683nm-pulsed laser with (>5mJ) and (<100MHz).**

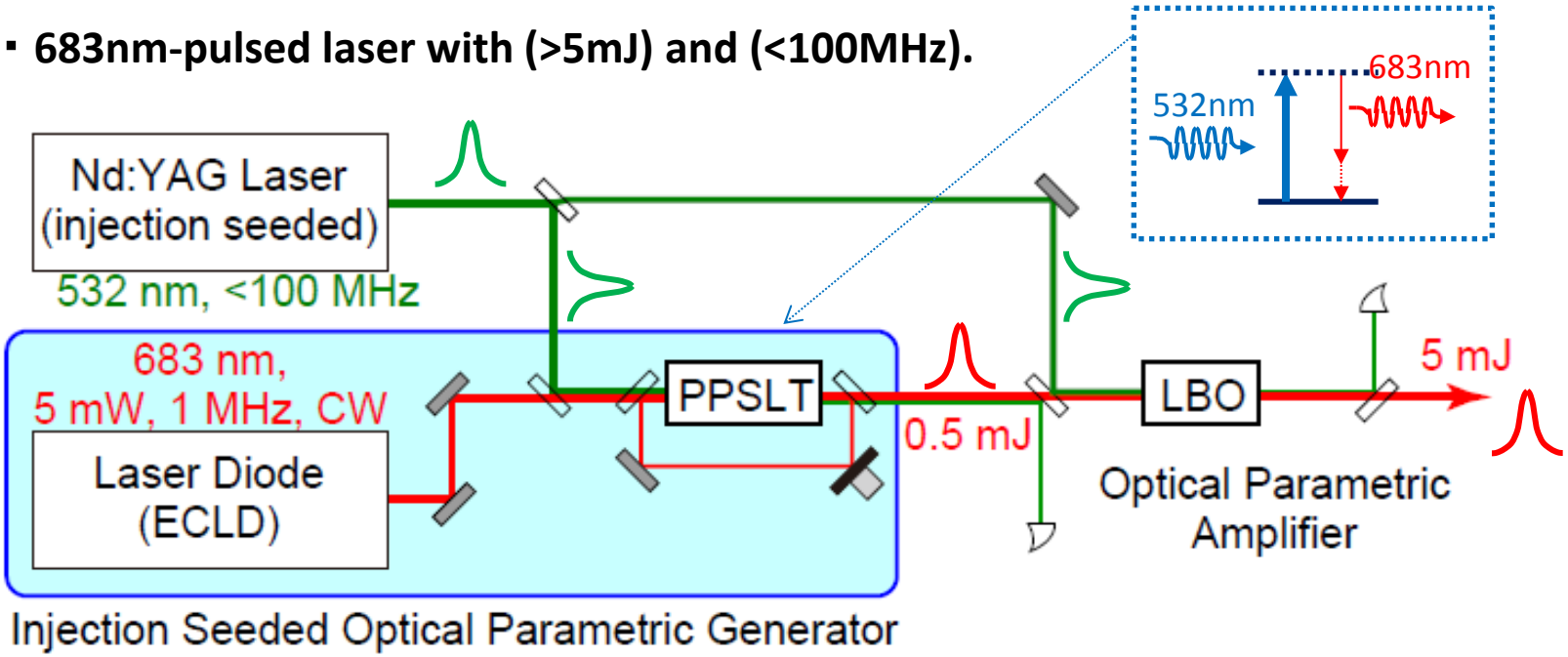

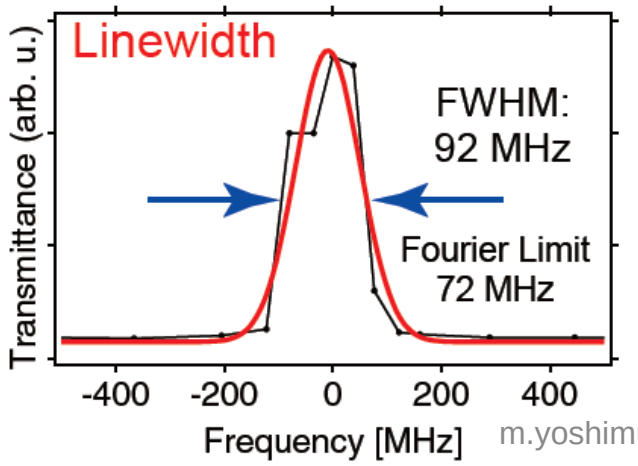

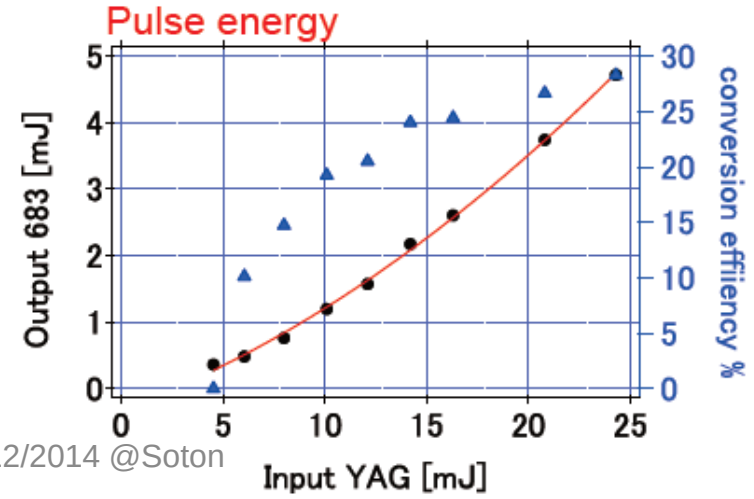

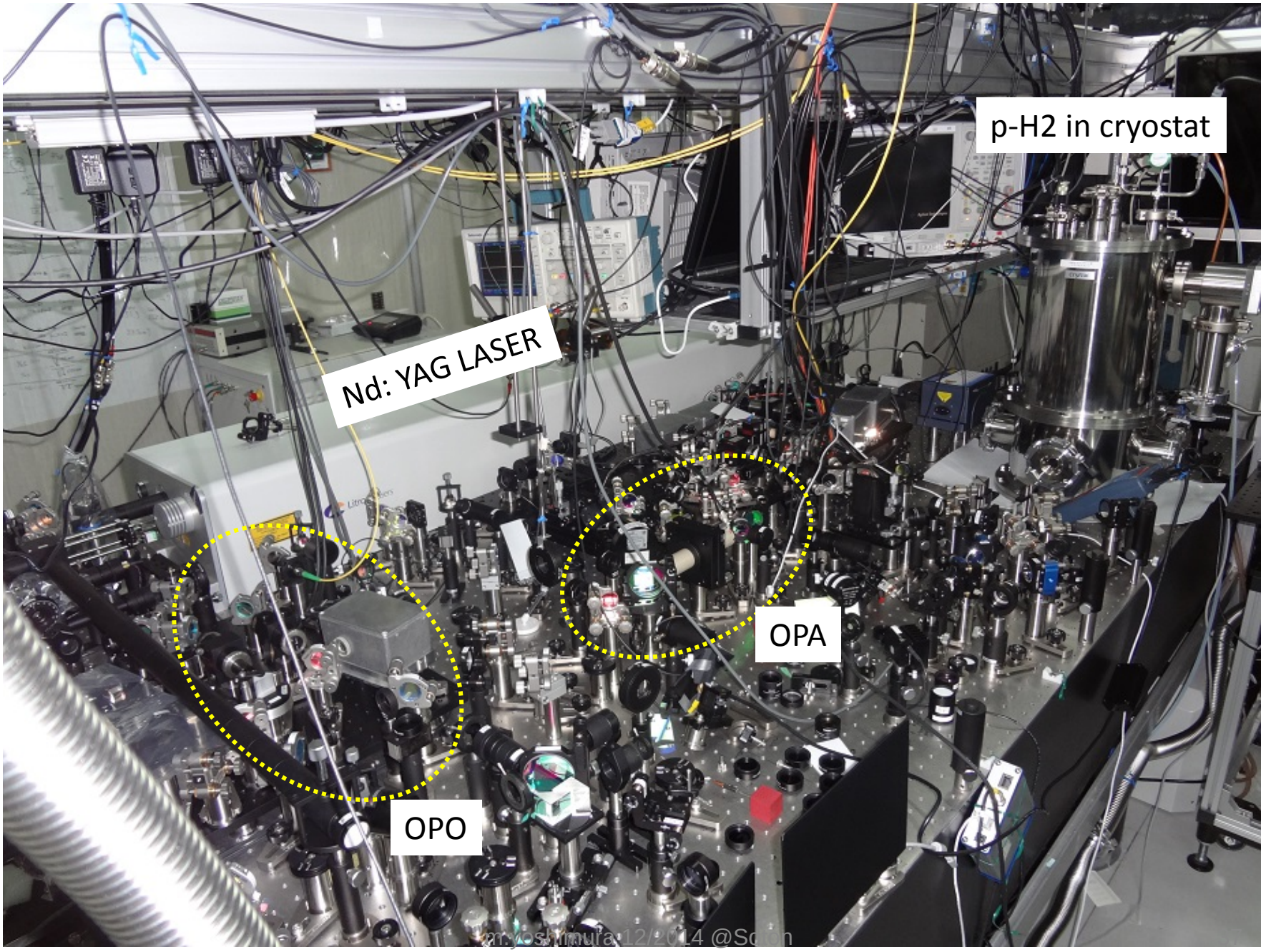
p-H2 in cryostat
Nd: YAG LASER
OPA
OPO

Observation of broadband Raman sidebands

- Raman sidebands, from 192 to 4662nm, are observed: >24
- Evidence of large coherence

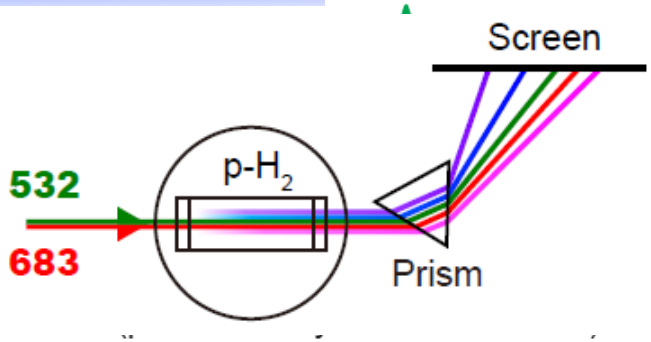

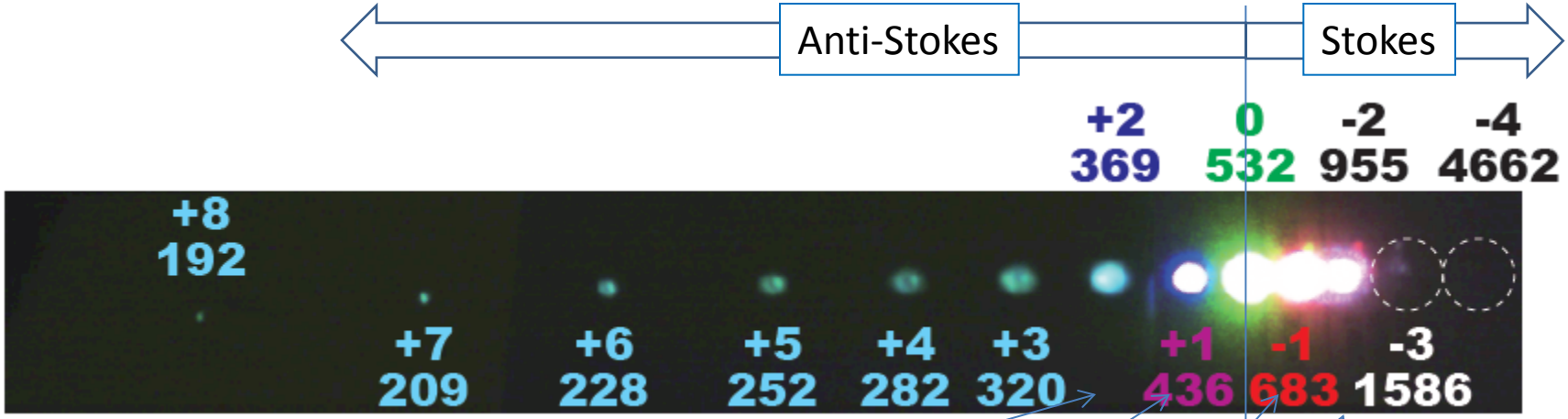

Without coherence

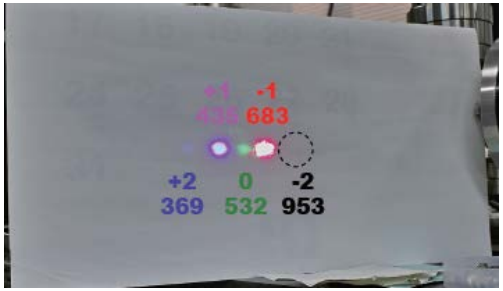

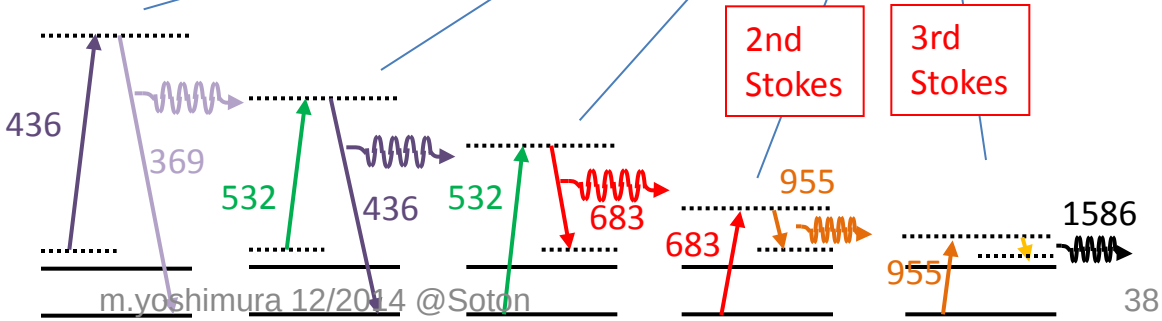

Coherence estimation

By comparing between measured power spectrum of sideband and numerical simulation (Maxwell-Bloch),

⇩

Coherence is estimated;
"Best fit"

$$\rho_{ge} \approx 0.032$$

Comparison of experiment and simulation for power spectrum of sideband

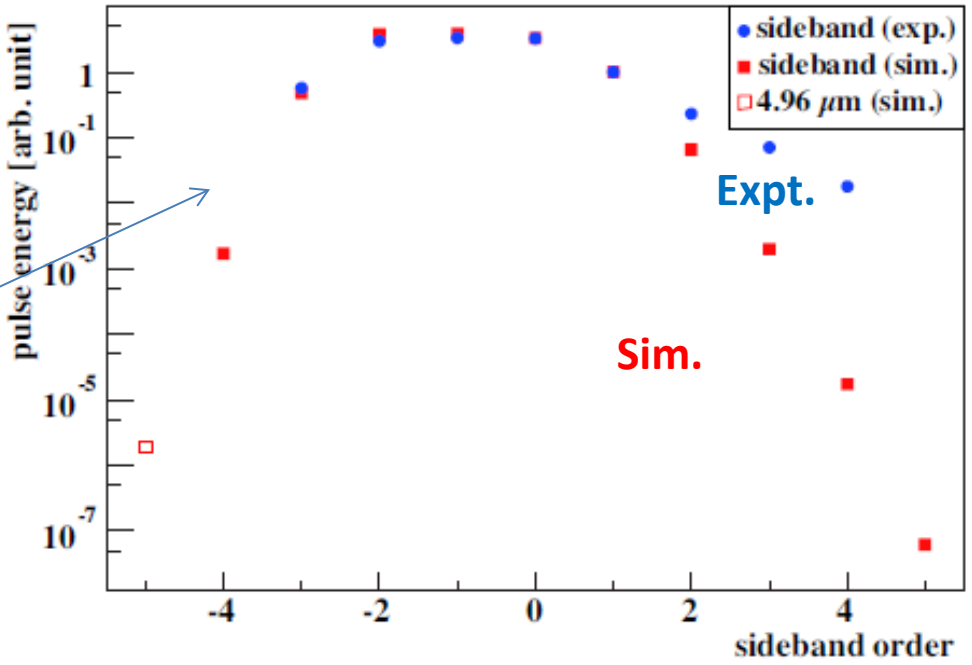

Maxwell-Bloch eq.

atom pol.

$$\frac{\partial \rho_{gg}}{\partial \tau} = i\left(\Omega_{ge}\rho_{eg} - \Omega_{eg}\rho_{ge}\right) + \gamma_1 \rho_{ee}$$

$$\frac{\partial \rho_{ee}}{\partial \tau} = i\left(\Omega_{eg}\rho_{ge} - \Omega_{ge}\rho_{eg}\right) - \gamma_1 \rho_{ee}$$

$$\frac{\partial \rho_{ge}}{\partial \tau} = i\left(\Omega_{gg} - \Omega_{ee} + \delta\right)\rho_{ge} + i\Omega_{ge}\left(\rho_{ee} - \rho_{gg}\right) - \gamma_2 \rho_{ge}$$

Fields

$$\frac{\partial E_q}{\partial \xi} = \frac{i\omega_q n}{2c}\left\{\left(\rho_{gg}\alpha_{gg}^{(q)} + \rho_{ee}\alpha_{ee}^{(q)}\right)E_q + \rho_{eg}\alpha_{eg}^{(q-1)}E_{q-1} + \rho_{ge}\alpha_{ge}^{(q)}E_{q+1}\right\}$$

$$\frac{\partial E_p}{\partial \xi} = \frac{i\omega_p n}{2c}\left\{\left(\rho_{gg}\alpha_{gg}^{(p)} + \rho_{ee}\alpha_{ee}^{(p)}\right)E_p + \rho_{eg}\alpha_{ge}^{(p\bar{p})}E_{\bar{p}}^{*}\right\}$$

PSR signal

The 4th stokes field can be used for PSR-trigger

4th stokes : λ = 4.662μm -> 0.266eV

→ 0.5 – 0.266eV = 0.234 eV (4.96μm) : PSR – signal !

Only component to trigger PSR

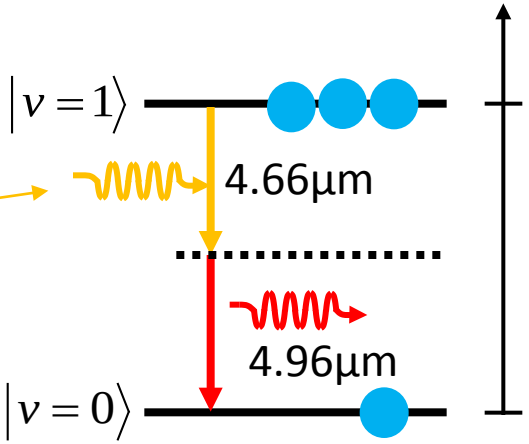

Observed PSR-signal (4.96μm)

- Monochromator and MCT-detector
- 4th Stokes (4.66μm) is suppressed by LPF
- 4.96μm is not affected by the LPF

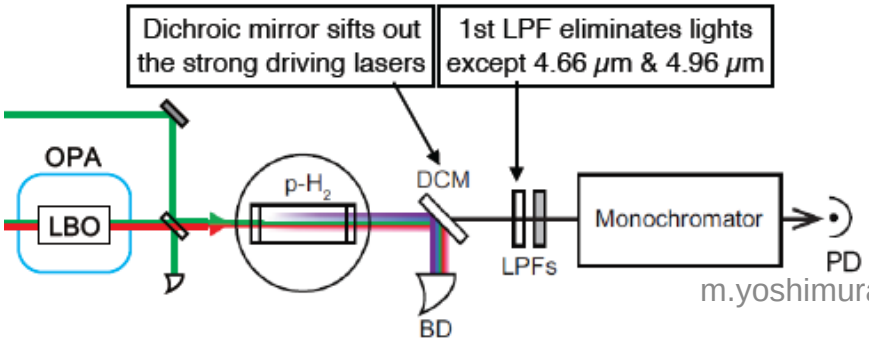

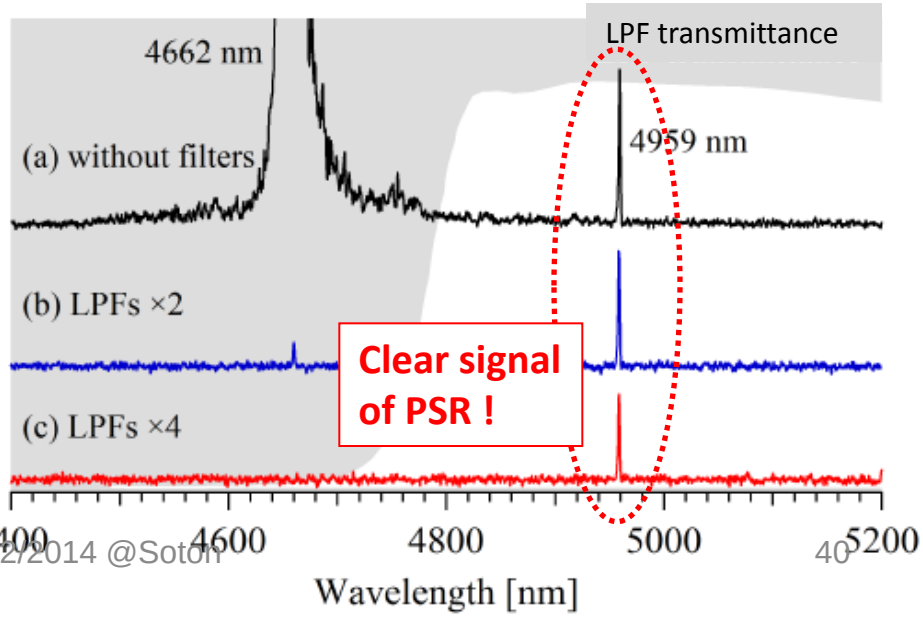

Enhancement of PSR rate

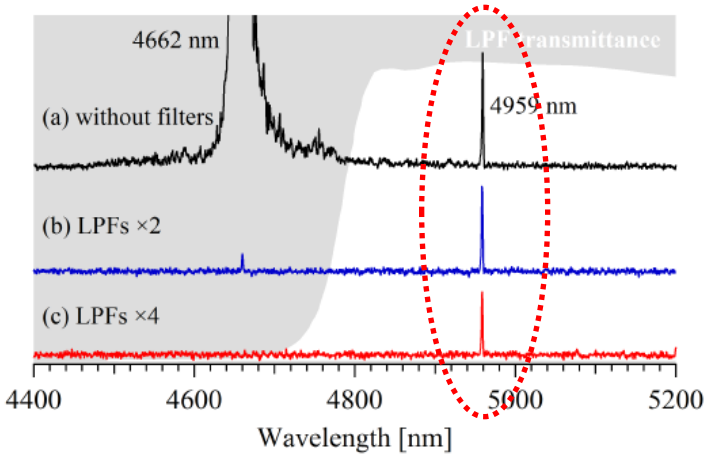

Measured 4.96μm energy

$$\sim 1.7\ \mathrm{pJ/pulse} \quad \left(4.4\times10^{7}\ \mathrm{photon}\right)$$

Spontaneous two-photon decay rate

$$\frac{dA}{dz}=\frac{\omega_{eg}^{7}}{(2\pi)^{3}c^{6}}\left|\alpha_{ge}^{(p\bar{p})}\right|^{2}z^{3}(1-z)^{2}\sim 3.2\times10^{-11}[/\mathrm{s}] \quad (z=\frac{1}{2})$$

$$n_0\approx 1.5\times10^{16},\ \frac{\Delta\Omega}{4\pi}\approx 1.2\times10^{-4},\ \Delta z\approx 4.9\times10^{-3},\ \Delta t\approx 80\,\mathrm{ns}$$

Photon number $= R_0\cdot\pi w_0^2 L n_0\cdot\frac{dA}{dz}\Delta z\cdot\frac{\Delta E}{E}\Delta t\approx 1.6\times10^{-8}$

Enhancement factor $=\dfrac{4.4\times10^{7}}{1.6\times10^{-8}}\approx10^{15}$

Order of 15 enhancement is only understood in the presence of macro-coherence

What to be done from now on

Twin process and controlled switching

RENP uses large medium polarization and stored fields by PSR, but two processes have different selection rules

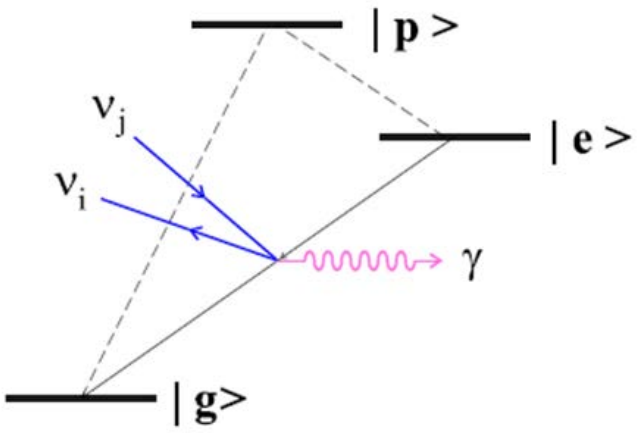

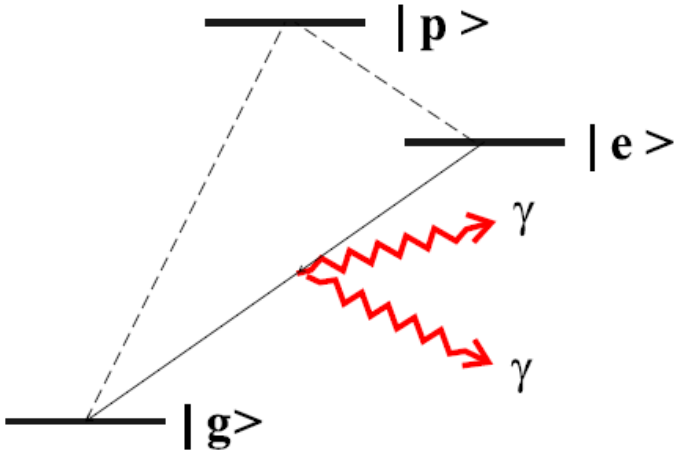

RENP: (E0 or M1)xE1

PSR: E1xE1

PSR-RENP switching is achieved by application of modulated E

Ideal state for RENP after PSR activity

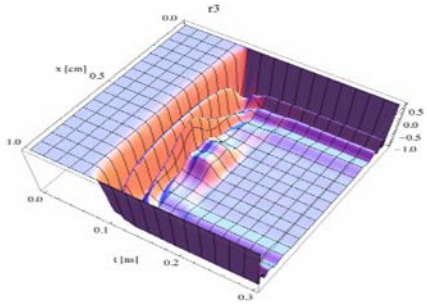

Figure 8: Spacetime profile of r_3 for the 1 Wmm^{-2} case of Fig(3).

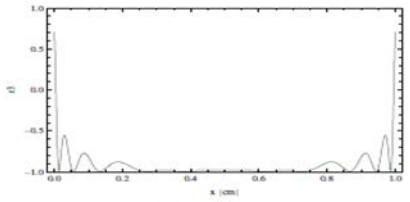

Figure 9: Spatial profile of r_3 at the latest time, 0.3 ns after trigger irradiation, of Fig(8).

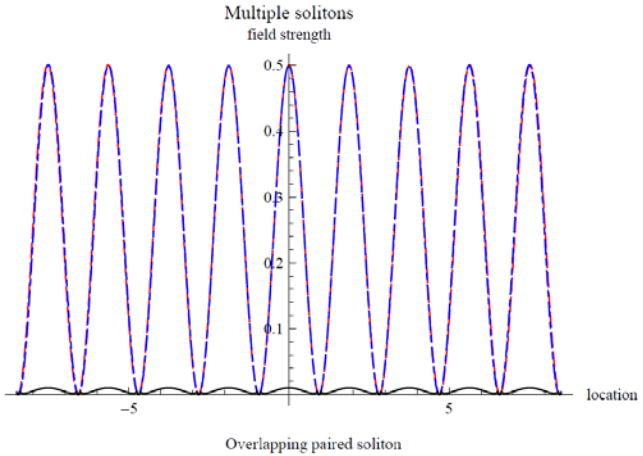

Soliton-condensates stable against two-photon emission, unstable for RENP

Analogue of
stopped light
polariton in cavity QED
Realized by two counter-propagating trigger PSR modes

Experimental strategy towards neutrino mass spectroscopy

- 1st stage: proof of macro-coherence principle using QED (PSR): we already achieved this stage, almost but not completely

- 2nd stage: control of PSR and soliton formation, switching between PSR and RENP modes, study of solid targets

- 3rd stage: discovery of the RENP process, measurements of mass matrix

Solid target: doped ions in ferro-electrics

- Large target number density required for PV measurements
- PSR <-> RENP mode switching effective
- Collaboration with specialists to be started

Summary

- Systematic neutrino mass spectroscopy is made possible when macro-coherence is realized. Controlled PSR by formation of soliton-condensate should be achieved.

- Since the macro-coherent QED process (PSR) has been experimentally observed, we go to the next stage towards RENP R&D.